Cloud Publications
International Journal of Advanced Remote Sensing and GIS
2014, Volume 3, Issue 1, pp. 433-445, Article ID Tech-188
ISSN 2320 - 0243

Cloud Publications

Research Article **Open Access**

Evaluating the Thermal Spatial Distribution Signature for Environmental Management and Vegetation Health Monitoring

Anibal Gusso[1,5], Mauricio Roberto Veronez[2], Fernanda Robinson[3], Vanessa Roani[3], and Rafaela Christ Da Silva[4]

[1]Department of Environmental Engineering, University of Vale do Rio dos Sinos (UNISINOS), São Leopoldo-RS, CP275, Brazil
[2]Graduate Program in Geology, University of Vale do Rio dos Sinos (UNISINOS), São Leopoldo-RS, CP275, Brazil
[3]Undergraduate Program in Environmental Management, University of Vale do Rio dos Sinos (UNISINOS), São Leopoldo-RS, CP275, Brazil
[4]Undergraduate Program in Geology, University of Vale do Rio dos Sinos (UNISINOS), São Leopoldo-RS, CP275, Brazil
[5]Center for Remote Sensing and Meteorological Researches, Federal University of Rio Grande do Sul (UFRGS), Porto Alegre, Brazil

Correspondence should be addressed to Anibal Gusso, anibalg@unisinos.br

Publication Date: 21 January 2014

Article Link: http://technical.cloud-journals.com/index.php/IJARSG/article/view/Tech-188

Guest Editor-in-Chief: Dr. Maurício Roberto Veronez
(This article belongs to the Special Issue "Application of Geotechnology in Urban Planning")

Abstract An accurate evaluation of the environment while cities are still growing economically is highly necessary for reliable assessment of ecosystem conditions. This research evaluates a comparison between the pattern of Land Surface Temperature (LST) distribution and Enhanced Vegetation Index 2 (EVI-2) during the summer season as an indicator of development conditions in an Area of Environmental Protection (AEP) that is under pressure from the surrounding urban environment in São Leopoldo, Brazil. A TSDS (Thermal Spatial Distribution Signature) procedure using Thermal infrared (TIR) data obtained from Landsat-5 Thematic Mapper (TM) was applied to evaluate vegetation coverage conditions. A set of six images were used to analyze vegetation development of an AEP between 1985 and 2009. Our analysis suggests that there is a strong relationship between the spatial distributions of LST and its pattern of vegetation coverage conditions. The LST variance exhibited differences in the two studied periods. A decreasing trend was observed in the variance averages from 1.04 to 0.35, which is associated to higher LST occurrences and a wider range of LST distribution in the first period than in the second. The results indicate that the LST distribution variance close to 1.0 can be associated with several level of vegetation degradation. In addition, a variance below 0.5, inside the studied AEP during summertime, is associated with better conditions of vegetation

coverage. In this manner, the TSDS procedure was considered a simple yet effective procedure for the timely diagnosis of AEP.
Keywords *Land Surface Temperature; TSDS; Remote Sensing; Area of Environmental Protection; Wetland; Vegetation Coverage*

1. Introduction

In the 19th century, civilization initiated a powerful transformation of land use cover without precedent that is strongly related to the high acceleration of industrialization. In recent decades, excessive local demands on environmental systems became global in scope (Brown, 2010). Since then, frequently, the processes of soil occupation have been demonstrated to be in disagreement with the concepts of sustainable development. In this scenario, legislative processes are an indispensable means for defining priority uses of land use (Fragomeni, 2005). However, the monitoring of local environmental problems and planning is perceived, increasingly, as an institutional and governmental tool to introduce the principles of sustainable development. The (SEMMAM Report, 2007) was established by the Administration of the São Leopoldo municipality and University of Vale do Rio dos Sinos to obtain a realistic diagnosis of environmental problems and soil occupation surveys in relevant Areas of Environmental Protection. Environmental problems herein refer to any human-induced damage to the physical environment inside Areas of Environmental Protection (AEP) but mainly indicate degradation of vegetated coverage resulting from estate pressure, unfair waste management or any other unintended side-effect due to human activity.

This research explores the development of a quantitative methodology for the evaluation of the general physical conditions of vegetated land cover based on the monitoring of Land Surface Temperature (LST) distribution in an AEP.

It is well known that shade trees and even small plants for land cover, such as shrubs and grass, help cool the urban environment (Bell et al., 2008). Furthermore, urban green space is always beneficial to mitigating urban heat islands and the evapotranspiration process generated by trees and vegetation in cities can cool the air by using the surrounding urban environment heat from the air to evaporate water (Li et al., 2011). The LST is closely related to the distribution of land use and land cover (LULC) characteristics (Weng et al., 2004; Gusso, 2013) and the physical conditions and properties of the vegetation types and surrounding urban environment are key factors that determine LST distribution (Chudnovsky et al., 2004).

The Landsat series satellites collected several years of data in the thermal spectral band, and the launch of LDCM (Landsat Data Continuity Mission) on February 11th, 2013, carrying the Thermal Infrared Sensor (TIRS), will extend the Land sat data archive from the earlier missions, thus allowing long-term studies (Irons et al., 2012).

A literature review has indicated that thermal satellites with high temporal resolution data are able to generate accurate classifications of environmental parameters (Kogan et al., 2002) and agricultural vegetation conditions (Silva et al., 2005; Gusso, 2013). This paper takes this method a step further, combining applicability of medium spatial resolution satellite imagery and providing an objective methodology for the monitoring of wetlands using thermal satellite data that can be used by decision makers and planners for environmental diagnosis. The objective in this work is to evaluate a LST-based procedure using medium resolution sensor images to obtain an accurate assessment of vegetation conditions in wetland AEPs. TSDS can assist the management of local and regional environmental protected areas further by providing reliable spatial information regarding natural vegetation conditions.

2. Study Area

This study covers an AEP of 445 ha located between the following coordinates (51º13'39"W, 29º49'48"S) and (51º01'14"W, 29º38'59"S) as shown in Figure 1. Approximately 72% of the wetlands in the state have an area smaller than 100 ha (Rolon and Maltchick, 2006). São Leopoldo has a total area of 10,700 ha, and it is located in a highly urbanized area in Rio Grande do Sul State (Figure 1). According to the (IBGE, 2012), the city has an estimated population of 193,403 inhabitants, with most of them (98%) located in the urban area.

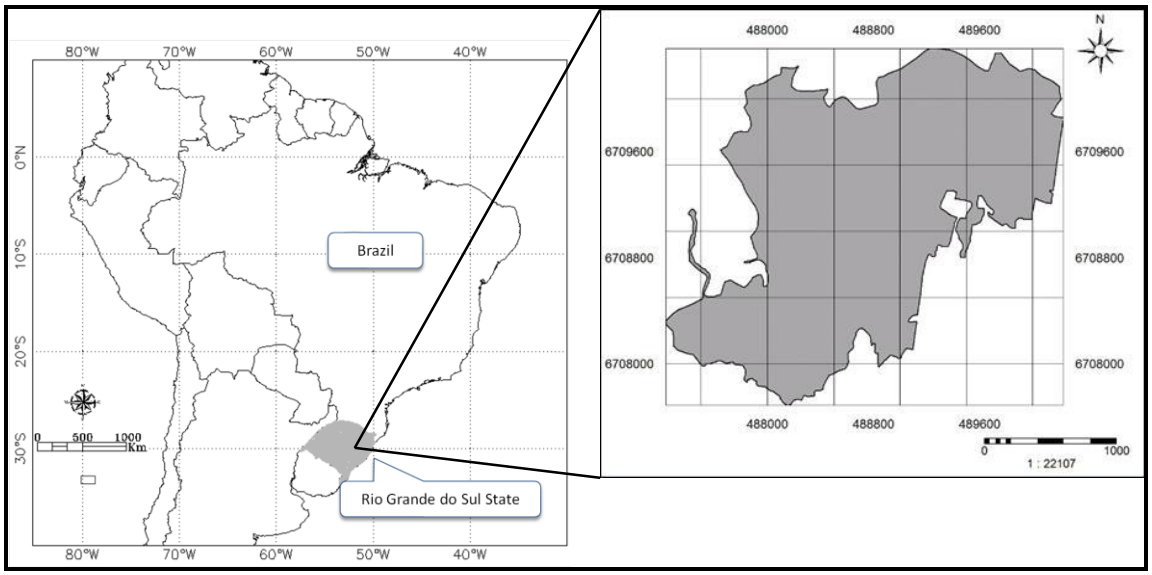

Figure 1: *São Leopoldo Municipality in Rio Grande do Sul State, Brazil, and the AEP*

São Leopoldo municipality is located in the lower part of the basin over an extensive plain configuration, consisting of wetlands and floodplains, and its economy is mainly based on the transformation industry, in particular the processing of leather for shoe manufacturers (Teixeira, 2002).

The municipality has an average elevation of 26 m above sea level and occupies approximately 2.95% of the drainage area at the Rio dos Sinos basin (Nascimento, 2001). A moist subtropical mid-latitude climate prevails in this region with four well-defined seasons and an average annual temperature of 19.7ºC, varying between 12 and 26°C, with an absolute minimum of -0.7°C and a maximum of 40.4°C. The accumulated average rainfall during the year is 1538 mm with no dry period (Köppen, 1948). The studied AEP is covered by Landsat scene path/row 221-081.

3. Material and Methods

3.1. Satellite Imagery and Data Set

The data sources used for the LST distribution analysis included the

i. Monthly rainfall data of three surrounding meteorological stations, covering the period (October to December), before satellite measurements in January obtained from the Database for Meteorological Research of the Instituto Nacional de Meteorologia (Brazil, 2013). These data were used to validate LST and EVI-2 occurrence.

ii. Climate logical normal of accumulated rainfall from October to December.

iii. Landsat-5 TM images distributed in Brazil by the Instituto Nacional de Pesquisas Espaciais (INPE: www.dgi.inpe.br).

iv. Shuttle Radar Topography Mission (SRTM) data, which was used to generate a slope map with 30 m spatial resolution, according to (Rabus et. al. 2003). These data were used to identify the proper location of wetlands inside the studied area.

v. Wetlands vegetation definition and classification according to IBGE was used to compare and evaluate the obtained results to the present natural vegetation.

vi. Thematic map with vector delineation available for AEP obtained from SEMMAM Project-Report.

vii. Geo location reference images from National Aeronautics and Space Administration-Global Land Survey (http://landsat.gsfc.nasa.gov/).

This is composed by cloud free images and geo-referencing metrics with good quality were used. This latter product was used to provide accurate geo-registration on a per-pixel-basis of the selected images as presented in Table 1.

Table 1: *Selected Landsat-5 TM Imagery for the Monitoring of the Studied Area*

Year	Path/Row	Data Quality
	221/081	
First Period		
1985	6February	Ok
1986	24 January	Ok
1991	6 January	Ok
Second Period		
2004	11 February	Ok
2007	2 January	Ok
2009	7 January	Ok

3.2. Imagery Calibration and Data Generation

The Landsat-5 TM images were fully calibrated and corrected to generate reflectance and LST values, according to Landsat Calibration Documents (Chander, 2009). Typically, correction includes atmospheric- and sensor-related parameters and thus leads to the derivation of physical units such as reflectance (Schroeder et.al. 2006). Considering the strict sense, full image correction involves both applications of absolute calibration coefficients for sensor and related parameters of atmospheric correction to derive estimates of surface reflectance (Chander, 2009). In this work, the first step was to convert the digital numbers (DN) into radiance and then to reflectance, according to the calibration parameters of (Rabus and Eineder, 2003) and LST (Markham and Barker, 1987). To accurately transform DN into reflectance, the images were also atmospherically corrected according to (Chavez, 1996) for which the data necessary to perform the atmospheric correction in the visible bands 1-5 can be obtained from the image itself (Sobrino et al., 2004). Variations of atmospheric conditions are spatially and temporally significant (Chander et al., 2009). Thus, as quality control, imagery data were submitted to atmospheric condition criteria, and water vapor content, which requires that no image have atmospheric contamination effects above 60 DN in the blue band, was used. Subsequently, reflectance's values from Bands 3 and 4 were used to generate EVI-2 data according to equation 1 from (Jiang et al., 2008).

EVI-2 is a two-band version of EVI that has been developed for sensors without a blue band (Jiang et al., 2008). It retains sensitivity and linearity as EVI for high LAI canopies but does not rely on the

usually poor quality blue band (Liu et al., 2012). According to the EVI-2 approach, although it is computed without a blue band, it remains equivalent to the EVI. In this way, EVI-2 calculation (Equation 1) can be used as an acceptable substitute of EVI over atmospherically corrected pixels (Jiang et al., 2008). NIR and Red are the obtained reflectance in the near-infrared and red bands of Landsat-5 TM, respectively.

$$EVI2 = 2.5 * \frac{NIR - Red}{NIR + 2.4 * Red + 1} \quad \text{Equation (1)}$$

For the thermal analysis, from band 6, after converting the digital numbers (DN) into absolute radiance values, LST is computed from at-satellite brightness temperatures (i.e., blackbody temperature) under the assumption of unity emissivity and using pre-launch calibration constants (Weng et al., 2009; Chander et al., 2009). Then, LST is corrected to non-unity surface emissivity according to the formulation of (Markham and Barker, 1987) which, however, does not perform corrections to atmospheric effects (absorption and emissions along path) because of the difficulty with estimating water vapor content from thermal detection in the mono-window band 6 (Qin et al., 2001; Ma et al., 2010). Further numerous factors need to be quantified to assess LST retrieval from satellite thermal data, including sensor radiometric calibrations (Wukelic et al., 1989), atmospheric correction (Cooper and Asrar, 1989; Chavez, 1996), surface emissivity correction (Allen et al., 2002) and physically driven conditions of land coverage (Gusso, 2013). The conversion of the detected thermal radiation to brightness temperature (Chander et al., 2009) is given by Equation 2. After that, LST is obtained by correcting radiating surface temperature to the surface emissivity (ε), which is the ratio of the thermal energy radiated by the surface to the thermal energy radiated by a blackbody at the same temperature (Allen et al., 2002). The accurate retrieval of LST from thermal spectral bands also requires an accurate estimate of emissivity from surface coverage (Gusso et al., 2007). The emissivity of the surface is controlled by factors such as water content, chemical composition, structure and roughness (Andersen, 1997). The emissivity ε depends on the Leaf Area Index (LAI) as given by Equation 3 (Allen et al., 2002) as follows:

$$LST = \frac{K2}{\ln\left(\frac{\varepsilon_{NB} * K1}{L} + 1\right)} \quad \text{Equation (2)}$$

$$\varepsilon_{NB} = 0.97 + 0.0033 * LAI \quad \text{Equation (3)}$$

Where LST is the emissivity-corrected surface temperature (Kelvin); K1 is the calibration constant 1 (607.76); K2 is the calibration constant 2 (1260.56); L is the blackbody radiance of thermal band 6, and ε_{NB} is the emissivity factor, which depends on surface coverage type. When LAI<3.0, ε_{NB} = 0.98 because increased water content in vegetation actually increases emissivity capacity.

3.3. TSDS Concept: LST and Biophysical Descriptors

The concept for the AEP assessment procedure developed in this study is referred to as Thermal Spatial Distribution Signature (TSDS). TSDS is based on the concept that vegetation mitigates higher values of LST occurrences; therefore, when considering the same study area, the impervious surface or degraded vegetation coverage leads to a wider range of temperatures distribution.

As a first approach, the vegetation index values of natural vegetation cover were evaluated during the summer season. Leaves and branches reduce the amount of solar radiation that reaches the area below the canopy of a tree or plant. In the summer season, generally 10 to 30 percent of the sun's energy reaches the area below a tree, with most of it being absorbed by leaves and used for photosynthesis and some being reflected back into the atmosphere. During the winter season, the

sunlight transmitted through a tree can be much wider— 10 to 80 percent— because trees losing their leaves allow more sunlight through (Huang et al., 1990).

For any surface material, certain internal properties, such as heat capacity, thermal conductivity and inertia, play important roles in governing the temperature of a body at equilibrium with its surroundings (Campbell, 2002).

Thermal responses for vegetation can be highly varied as a function of the biophysical properties of the vegetation itself as well (Bottyán and Unger, 2003; Weng et al., 2004). These thermal properties vary with soil type and moisture content (Sandholt et al., 2002). Dry, bare, and low-density soils, for example, have been linked to high LST as a result of relatively low thermal inertia (Sandholt et al., 2002). This is because the emissivity of soils, or sparsely vegetated areas, is a function of soil moisture conditions and soil density (Valor and Caselles, 1996; Gusso et.al., 2007).

In surface areas characterized by fraction of vegetation cover, thermal properties from non-vegetated surface areas can largely influence the surrounding measurements of LST through the thermal processes related to direct interception of sunlight. In this way, it is expected that degraded or sparsely vegetated areas are not able to cool the surrounding sensible heat by means evapotranspiration, which leads to a spread in the range of LST occurrences by increasing statistical indicators in terms of the variance of distribution toward higher LST values in a histogram. Thus, in this study, we only used summer season imagery to detect the most pronounced values of LST because of the heating effect associated with surface coverage.

The LST obtained from satellite imagery is, strictly speaking, a measure of “skin” temperature or surface radiometric energy (kinetic) emitted from the land surface and is related to the thermal infrared (TIR) radiation rather than air temperature (Qin et al., 2001; Gusso et al., 2007), which is more commonly used in physiological studies (Sims et al., 2008). The relationship between thermal characteristics of surface and vegetation indices has been extensively documented in the literature (Nemani et al., 1993; Lambin & Ehrlich, 1996; Sandholt et al., 2002; Kogan et al., 2002; Sims et al., 2008; Schelenker and Roberts, 2009; Carmo-Silva et al., 2012; Gusso, 2013).

The LST and vegetation index relationship has been used by (Kogan et al., 2002) for studies of the role of LST in global vegetation coverage dynamics and precipitation. (Lambin and Ehrlich, 1996) have used the relationship to analyze land cover dynamics with correlations between NDVI, brightness temperature and precipitation over the globe, and (Gusso, 2013) used it to evaluate drought impacts over agriculture in Rio Grande do Sul State, Brazil.

Many studies have observed a negative relationship between LST and vegetation indices. In the USA, (Nemani et al., 1993) used remotely sensed data to estimate surface moisture and identified a strong negative relationship between NDVI and LST over all present biomes, including grassland and forests. Given this and considering that temperature is closely related to physiological activities of vegetation cover, LST can be a useful measure of physiological activity of the top canopy leaves when leaf cover is great enough to not be affected by soil surface temperature (Sims et al., 2008).

Typically, simplified models that describe Land Use and Cover Change (LUCC) can provide a link between LST and physical spatial distribution. However, further statistical analysis plays an important role in linking LST to the surface characteristics (Bottyán and Unger, 2003). In addition, LST is highly variable through time, which does not allow comparing absolute values in a simplified conceptual approach. It is important to note that the studied AEPs in the early period (in the 1980s) were under different physically driven conditions of surface and vegetation coverage as compared with the most recent period. In this context, the challenge in the monitoring of environmental system is the same proposed by (Wilson et al., 2003), who searched for evidence of “to what extent changes in vegetation

vigor and surrounding physical conditions detected by remote sensing can actually reveal the natural environment conditions?" Using this conceptual approach, the TSDS procedure consists of the analysis and interpretation of statistical data associated to LUCC that leads to spatial and temporal variation of LST distribution.

3.4. Validation of TSDS

In this validation step, to partially determine the LST relation to biophysical descriptors, we compared LST values on a per-pixel-basis to EVI-2 data. The performance of the TSDS was validated by means of the analysis of LST distribution in relation to the vegetation index EVI-2 data. This analysis relates the LST to the vegetated land coverage capacity to perform evapotranspiration processes.

It is well-known that in drought-free years, well-developed vegetation reflects only a small portion of incident solar radiation in the visible band of spectrum because of chlorophyll absorption properties and other plant pigments that absorb sunlight (Gusso and Ducati, 2012). In the NIR, plants reflect much more because of a scattering effect caused by the internal structure and water content of leaves (Jensen, 2007).

By considering the bioclimatic conditions of natural vegetation cover in wetland areas, it became clear that the challenge is to understand what represents vegetation development, as it is expected that soil moisture tends to produce different spectral behavior in the reflectance bands. Background contamination can actually promote imbalance in the relation between bands 3 and band 4 (EVI-2 calculation), potentially leading to decreases in the resulting EVI-2 values under the influence of wetland areas. Thus, we compared accumulated rainfall to the climatologically normal data in the period from October to December, before satellite measurements (in January), to detect river flood occurrences that could result in low EVI-2 values from one period to another, masking the actual vegetation coverage conditions.

Figure 2 presents the rainfall deviation from the climatologically normal inside the AEP in 1984 and 2006, which is related to Landsat images on February 6, 1985 (first period), and January 2, 2007 (second period), respectively, indicating that soil moisture conditions in the different studied periods are similar. Rainfall data also indicate a slight water deficit for both periods (1984 and 2006), which reduces the possibility of a trend effect of background contamination from soil moisture.

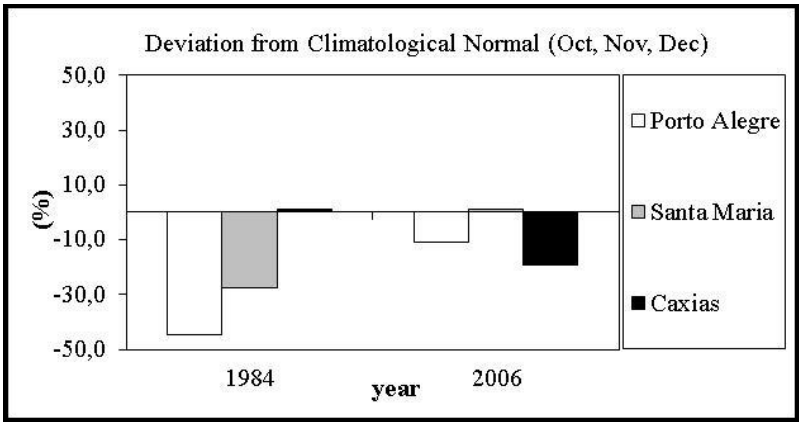

Figure 2: *Deviation from Climatologically Normal of Accumulated Rainfall in the Period October to December of 1984 and 2006*

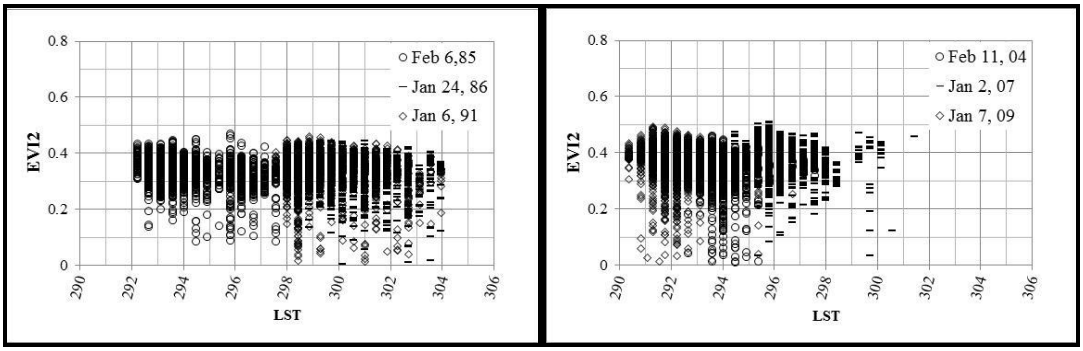

Figure 3: *Scatter gram of LST against EVI-2 from Landsat-5 TM Covering the Area of Environmental Protection in the (A) First Period and (B) Second Period*

4. Results and Discussion

The validation step, which compares the obtained results of TSDS estimates with obtained from EVI-2 for natural vegetation cover evaluation, indicated that the two estimates are in good agreement. The distribution of LST and EVI-2 inside the AEP, as shown in Figure 3, revealed a wider range of LST in the first period than in second one. This result is in agreement with the expected inverse mathematical relation based on the physical assumption that LST and EVI-2 data, at a given pixel, vary inversely over time.

Regarding the LST distribution, in the first period, LST is distributed from 292 to 304 Kelvin (ΔLST= 12 K), whereas in the second period, most of the data are between 290 and 298 Kelvin (ΔLST= 8K), as shown. Although daily weather variations of temperatures can actually mask the range of LST distribution, a slight increase in the EVI-2 values reaching 0.5 units is associated with the second period in Figure 3, which also suggests a slight improvement in vegetation health coverage.

Figure 4 presents bar-chart diagrams for the six dates monitored for the AEP between 1985 and 2009. It is also important to note that intra-period variances are in agreement. The variance values were between 1.11 and 0.95, in the first period, and between 0.27 and 0.39 in the second period, as shown in Figure 5. This result indicates that the LST distribution adheres to the evaluated physical concept of vegetation coverage in the two different studied periods. The average of variances obtained from LST distribution analysis is 1.04 in the first period and 0.35 in the second period. It is possible to observe in Figure 4a, 4c and 4e a specific configuration of LST distribution characterized by a bimodal distribution. These results indicate that the LST distribution variance is close to 1.0 in the studied AEP during summertime and can be associated with some level of vegetation degradation. In addition, a variance below 0.5 is associated with better vegetation coverage conditions.

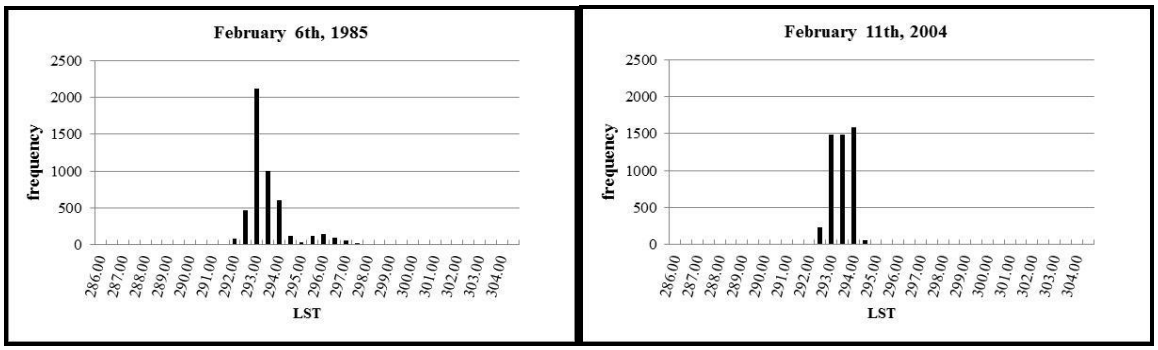

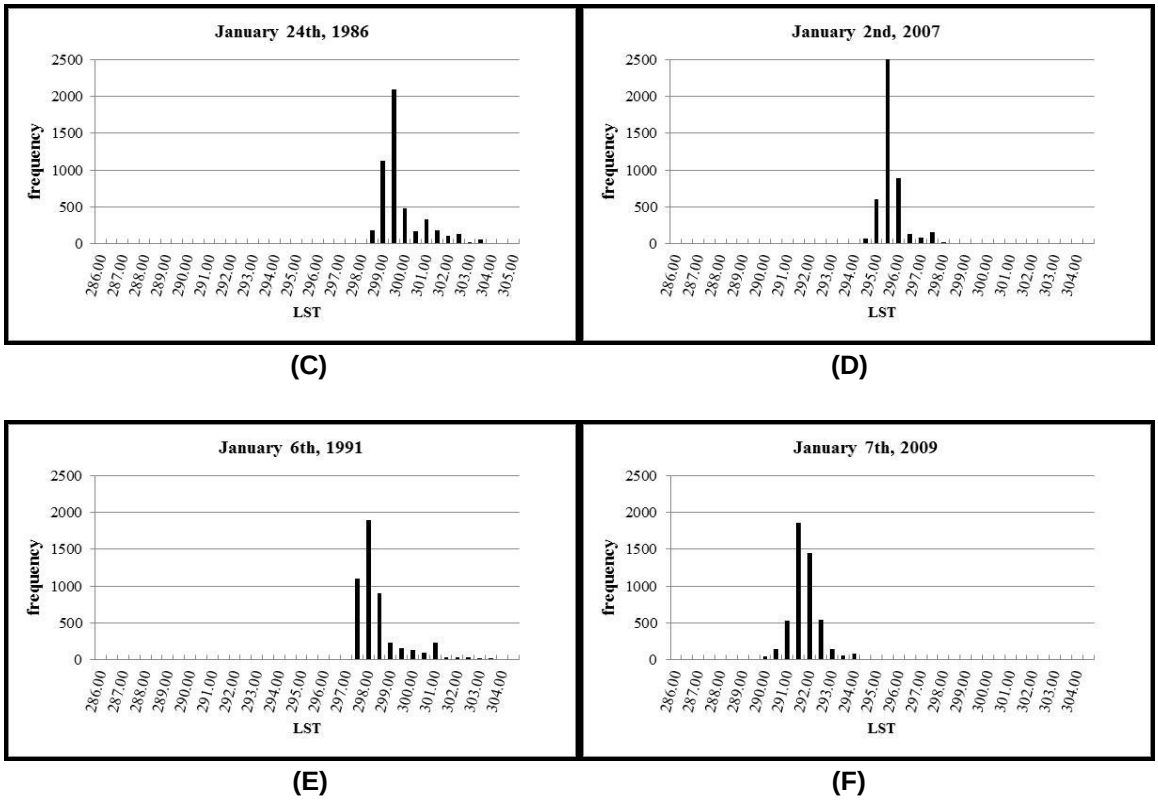

Figure 4: *Estimated LST Distribution in the AEP for the First Period (A, C, E) and the Second Period (B, D, F)*

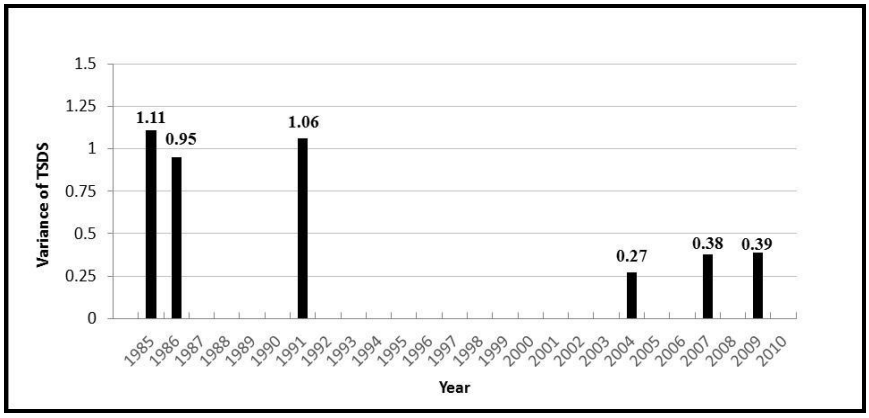

Figure 5: *Variance of LST Distribution inside the AEP in the Two Periods from 1985 to 2009*

5. Conclusion

The analysis of vegetation coverage conditions using the LST distribution indicated that in the first period, a wider range of LST is associated with higher fractions of impervious surfaces or degraded vegetation conditions. The results indicate that LST distribution variance below 0.5, inside the studied AEP during summertime, is associated with better vegetation coverage conditions. In addition, a variance close to 1.0 can be associated with some level of vegetation degradation. Thus, the TSDS procedure based on LST distribution analysis was demonstrated to be an objective and consistent methodology for the evaluation of the general vegetation coverage conditions inside Areas of Environmental Protection.

Our results suggest that the vegetation conditions and AEP coverage grew substantially after January 6, 1991. Because of the simplified analysis process used in TSDS and the computation resources needed, it is a timesaving procedure and is less vulnerable to analyst image interpretation skills and subjectivity.

This study also demonstrates that even when not considering geological and pedological questions in the study as related to estate pressure, the municipality urban development appears to be in agreement with the AEPs boundaries even before the implementation of the State Law Code for Environment in Rio Grande do Sul defined on August 3, 2000 (*CódigoEstadual de MeioAmbiente do Estado do Rio Grande do Sul – Lei Estadual nº 11.520, de 3 de agosto de 2000*), as there was no detected expansion toward the studied AEP.

Finally, the TSDS procedure is not species-specific and is therefore useful for application to the analysis of several other vegetation types. We expect that the use of TSDS analysis applied to another ecoregions, under different natural vegetation conditions and climate, can generate good results. In this context, the launch of the LDCM (Landsat Data Continuity Mission) on February 11, 2013, and TSDS can further assist the management of local and regional environmental protected areas by providing reliable spatial information on natural vegetation conditions.

Acknowledgments

We wish to thank the Vale do Rio dos Sinos University (UNISINOS) and National Aeronautical and Space Administration (NASA) for the Landsat-5 TM data and the Image Processing Division at the Instituto Nacional de Pesquisas Espaciais (INPE) for the Landsat-5 TM data distribution in Brazil. We also wish to specially thank the Conselho Nacional de DesenvolvimentoCientífico e Tecnológico (CNPq) for their support.

References

Brown L. *World on the Edge*. W. W. Norton & Company. 2010. 325.

Fragomeni A.L.M. *Parques Industriais Ecológicos como Instrumento de Planejamento e Gestão Ambiental Cooperativa.* 2005.

SEMMAM-Report. *Implantação De Um Sistema De Informação Geográfica Como Ferramenta No Diagnóstico Ambiental Do Município De São Leopoldo/RS*. 2007. 14.

Bell R., et al. *Reducing Urban Heat Islands: Compendium of Strategies-Trees and Vegetation.* 2008.

Li J., et al. *Impacts of Landscape Structure on Surface Urban Heat Islands: A Case Study of Shanghai, China.* Remote Sensing of Environment. 2011. 115; 3249-3263.

Weng Q., et al. *Estimation of Land Surface Temperature–Vegetation Abundance Relationship for Urban Heat Island Studies.* Remote Sensing of Environment. 2004. 89; 467-483.

Gusso A. *Integração de Imagens NOAA/AVHRR: Rede de Cooperação para Monitoramento Nacional da Safra de Soja*. Rev. Ceres [Online]. 2013. 60 (2) 194-204.

Chudnovsky A., et al. *Diurnal Thermal Behavior of Selected Urban Objects using Remote Sensing Measurements.* Energy and Buildings. 2004. 36 (11) 1063-1074.

Irons J.R., et al. *The Next Landsat Satellite: the Landsat Data Continuity Mission*. Remote Sensing of Environment. 2012. 122; 11-21.

Kogan F.N. *World Droughts in the New Millennium from AVHRR-based Vegetation Health Indices*. Eos Trans. 2002. 83; 557-564.

Silva B.B., et al. *Balanço De Radiação Em Áreas Irrigadas Utilizando Imagens Landsat 5–TM*. Revista Brasileira de Meteorologia. 2005. 20 (2) 243-252.

Rolon A.S. and Maltchik L. *Environmental Factors as Predictors of Aquatic Macrophyte Richness and Composition in Wetlands of Southern Brazil*. Hydrobiologia. 2006. 556; 221-231.

Nascimento C.E.G. *Verificação De Critérios Técnicos Para Seleção De Áreas Aptas A Disposição Final De Resíduos Sólidos Urbanos No Município De São Leopoldo–RS.* 2001.

Teixeira M.B. *Plano Ambiental De São Leopoldo: Estruturas Institucionais, Legislação, Planejamento E Proteção Ambiental*. MTC. 2002. 1; 128.

Köppen W. *Climatologia: con un Estúdio de los Climas de la Tierra*. Fondo de Cultura Econômica. 1948. 466.

IBGE–Instituto Brasileiro de Geografia e Estatística. http://www.ibge.gov.br/english/ (accessed on July 2nd, 2012).

Rabus B.M. and Eineder A.R.R. *The Shuttle Radar Topography Mission—a New Class of Digital Elevation Models Acquired by Space Borne Radar*. Photogram. Eng. Remote Sensing. 2003. 57; 241-262.

Chander G., et al. *Summary of Current Radiometric Calibration Coefficients for Landsat MSS, TM, ETM+, and EO-1 ALI Sensors.* Remote Sens. Environ. 2009. 113; 893-903.

Schroeder et al. *Radiometric Correction of Multi-Temporal Landsat Data for Characterization of Early Successional Forest Patterns in Western Oregon.* Remote Sensing of Environment. 2006. 103; 16-26.

Markham B.L. and Barker J.L. *Thematic Mapper Band pass Solar Exoatmospherical Irradiances.* Int. Journal of Remote Sensing. 1987. 8 (3) 517-523.

Chavez Jr. P.S. *Image-Based Atmospheric Correction—Revisited and Improved.* Photogram. Eng. Remote Sensing. 1996. 62; 1025-1036.

Sobrino J.A., et al. *Land Surface Temperature Retrieval from LANDSAT TM 5.* Remote Sensing of Environment. 2004. 90 (4) 434-440.

Jiang Z., et al. *Development of a Two-Band Enhanced Vegetation Index without a Blue Band*. Remote Sensing of Environment. 2008. 112; 3833-3845.

Liu et al. *Assessment of Vegetation Indices for Regional Crop Green LAI Estimation from Landsat Images over Multiple Growing Seasons.* Remote Sensing of Environment. 2012. 123; 347-358.

Weng Qi. *Thermal Infrared Remote Sensing for Urban Climate and Environmental Studies: Methods, Applications, and Trends.* ISPRS Journal of Photogrammetric and Remote Sensing. 2009. 64; 335-344.

Qin Z., et al. *A Mono-Window Algorithm for Retrieving Land Surface Temperature from Landsat TM Data and its Application to the Israel–Egypt Border Region.* International Journal of Remote Sensing. 2001. 22 (18) 3719-3746.

Ma Y., et al. *Coupling Urbanization Analyses for Studying Urban Thermal Environment and its Interplay with Biophysical Parameters Based on TM/ETM+ Imagery.* 2010.

Wukelic G.E., et al. *Radiometric Calibration of Landsat Thematic Mapper Thermal Band.* Remote Sensing of Environment. 1989. 28; 339-347.

Cooper D.I. and Asrar G. *Evaluating Atmospheric Correction Models for Retrieving Surface Temperatures from the AVHRR Over A Tall Grass Prairie*. Remote Sensing of Environment. 1989. 27; 93-102.

Allen R.G., et al. *Surface Energy Balance Algorithms for Land (SEBAL)*. Advanced Training and User´s Manual. 2002. 1; 97.

Gusso A., et al. *Mapeamento Da Temperatura Da Superfície Terrestre Com Uso Do Sensor NOAA/AVHRR.* Pesquisa Agropecuária Brasileira. 2007. 42; 231-237.

Andersen H.S. *Land Surface Temperature Estimation Based on NOAA-AVHRR Data during the HAPEX-Sahel Experiment*. Journal of Hydrology. 1997. 189; 788-814.

Huang J., et al. *The Wind-Shielding and Shading Effects of Trees on Residential Heating and Cooling Requirements. ASHRAE Winter Meeting*. American Society of Heating, Refrigerating and Air-Conditioning Engineers. 1990.

Campbell J.B. *Introduction to Remote Sensing*. The Guilford Press. 2002. 3.

Bottyán Z. and Unger J. *A Multiple Linear Statistical Model for Estimating the Mean Maximum Urban Heat Island.* Theoretical and Applied Climatology. 2003. 75 (3-4) 233-243.

Sandholt L., et al. *A Simple Interpretation of the Surface Temperature/Vegetation Index Space for Assessment of Surface Moisture Status.* Remote Sensing of Environment. 2002. 79; 213-224.

Valor E. and Cassells V. *Mapping Land Surface Emissivity from NDVI: Application to European, African, and South American Areas.* Remote Sensing of Environment. 1996. 57 (3) 167-184.

Sims D.A., et al. *A New Model of Gross Primary Productivity for North American Ecosystems Based Solely on the Enhanced Vegetation Index and Land Surface Temperature from MODIS*. Remote Sensing of Environment. 2008. 112; 1633-1646.

Nemani R., et al. *Developing Satellite-Derived Estimates of Surface Moisture Status*. Journal of Applied Meteorology. 1993. 32; 548-557.

Lambin E.F. and Ehrlich D. *Combining Vegetation Indices and Surface Temperature for Land-Cover Mapping at Broad Spatial Scales*. International Journal of Remote Sensing. 1995. 16; 573-579.

Schlenker W. and Roberts M. *Nonlinear Temperature Effects Indicate Severe Damages to U.S. Crop Yields Under Climate Change.* Proceedings of the National Academy of Sciences. 2009. 106; 15594-15598.

Carmo-Silva A.E., et al. *Decreased CO_2 Availability and Inactivation of Rubisco Limit Photosynthesis in Cotton Plants under Heat and Drought Stress in the Field*. Environmental and Experimental Botany. 2012. 83; 1-11.

Wilson et al. *Evaluating Environmental Influences of Zoning in Urban Ecosystems with Remote Sensing.* Remote Sensing of Environment. 2003. 86; 303-321.

Gusso and Ducati. *Algorithm for Soybean Classification Using Medium Resolution Satellite Images.* Remote Sens. 2012. 4; 3127-3142.

Jensen J.R. *Remote Sensing of the Environment: An Earth Resource Perspective*. 2007. 592.

National Aeronautics and Space Administration–NASA. *Landsat Data*. http://landsat.gsfc.nasa.gov/ (accessed on 5 December 2011).

Brazil, Banco de Dados Meteorológicos para Ensino e Pesquisa do Instituto Nacional de Meteorologia (BDMEP-INMET). http://www.inmet.gov.br/portal/index.php?r=bdm ep/bdmep (accessed on 30th March 2013).